Hematopoietic Stem Cell Regeneration Enhanced by Ectopic Expression of ROS-detoxifying Enzymes in Transplant Mice

Weimin Miao[1], Richard XuFeng[2], Moo-Rim Park[2,3], Haihui Gu[1,2,4], Linping Hu[1], Jin Wook Kang[1,2], Shihui Ma[1], Paulina H Liang[2], Yanxin Li[1,2], Haizi Cheng[2], Hui Yu[2], Michael Epperly[2], Joel Greenberger[2] and Tao Cheng[1,2]

[1]State Key Laboratory for Experimental Hematology, Institute of Hematology & Blood Diseases Hospital, Center for Stem Cell Medicine, Chinese Academy of Medical Sciences and Peking Union Medical College, Tianjin, China; [2]Department of Radiation Oncology and University of Pittsburgh Cancer Institute, University of Pittsburgh School of Medicine, Pittsburgh, Pennsylvania, USA; [3]Department of Internal Medicine, Wonkwang University School of Medicine, Iksan, Korea; [4]Department of Blood Transfusion, Changhai Hospital, Shanghai, China

High levels of reactive oxygen species (ROS) can exhaust hematopoietic stem cells (HSCs). Thus, maintaining a low state of redox in HSCs by modulating ROS-detoxifying enzymes may augment the regeneration potential of HSCs. Our results show that basal expression of manganese superoxide dismutase (MnSOD) and catalase were at low levels in long-term and short-term repopulating HSCs, and administration of a MnSOD plasmid and lipofectin complex (MnSOD-PL) conferred radiation protection on irradiated recipient mice. To assess the intrinsic role of elevated MnSOD or catalase in HSCs and hematopoietic progenitor cells, the MnSOD or catalase gene was overexpressed in mouse hematopoietic cells *via* retroviral transduction. The impact of MnSOD and catalase on hematopoietic progenitor cells was mild, as measured by colony-forming units (CFUs). However, overexpressed catalase had a significant beneficial effect on long-term engraftment of transplanted HSCs, and this effect was further enhanced after an insult of low-dose γ-irradiation in the transplant mice. In contrast, overexpressed MnSOD exhibited an insignificant effect on long-term engraftment of transplanted HSCs, but had a significant beneficial effect after an insult of sub-lethal irradiation. Taken together, these results demonstrate that HSC function can be enhanced by ectopic expression of ROS-detoxifying enzymes, especially after radiation exposure *in vivo*.

Received 5 December 2011; accepted 9 October 2012; advance online publication 8 January 2013. doi:10.1038/mt.2012.232

INTRODUCTION

While reactive oxygen species (ROS) is traditionally considered a toxic by-product of cellular metabolism, studies have shown that ROS play a central role as second messengers in the signal transduction of many cell types, including hematopoietic stem cells (HSCs).[1–4] ROS can also influence cell cycle progression depending upon the amount of ROS.[5–7] HSCs and their niche were shown to be predominantly located at the lowest end of an oxygen gradient in the bone marrow (BM), with the implication that regionally defined hypoxia plays a fundamental role in regulating stem cell function.[8] Jang and colleagues demonstrated that low-oxygen niche-derived HSCs, isolated indirectly based upon their low level of intracellular ROS expression, had a higher self-renewal potential than their high ROS counterparts.[9] Moreover, in *Atm*- or *FoxO*-deficient mice, HSCs were exhausted due to increased ROS levels,[10–13] and treatment with the antioxidative agent, N-acetyl-L-cysteine, resulted in reversion of the *Atm*- or *FoxO*-deficient HSC phenotype. Multiple lines of evidence have shown that ROS, which may be caused by ionizing radiation, are destructive to HSCs.[4,14,15] Our recent studies demonstrated that ROS generated in irradiated hosts may also pose a significant negative "bystander" effect on transplanted HSCs.[16] These results suggest that low physiological levels of ROS are beneficial for maintaining HSC function, while deregulated increases of ROS can cause defects in HSC repopulation.

Excessive intracellular ROS are scavenged by antioxidant enzymes, such as superoxide dismutase (SOD), which converts superoxide anion radicals (O_2^-) into hydrogen peroxide (H_2O_2) that can then be detoxified into water by catalase[17] and glutathione peroxidase.[18] There are three forms of SOD in eukaryotic cells: a copper- and zinc-containing enzyme (CuZnSOD, SOD1) found in the cytoplasm and nucleus,[19] a manganese-containing enzyme (MnSOD, SOD2) present in mitochondria,[20] and an extracellular form (EC-SOD, SOD3).[21] Mitochondria are a major source of intracellular ROS generation and previous studies investigating the effects of overexpressing MnSOD to decrease mitochondrial ROS have yielded diverse results. Overexpression of MnSOD was shown to prevent oxidative stress-induced apoptosis in two hematopoietic cell lines, 32Dcl3 and K562, and in primary murine BM cells.[22–24] However, in NIH/3T3 cells, MnSOD overexpression decreased cell growth.[6,7] Meanwhile, MnSOD was

**The first three authors contributed equally to this work.*

Correspondence: *Tao Cheng, Department of Radiation Oncology and University of Pittsburgh Cancer Institute, University of Pittsburgh School of Medicine, 5117 Centre Ave, Pittsburgh, Pennsylvania 15213, USA. E-mail: chengt@upmc.edu*

shown to provide significant radioprotection to cultured cells *in vitro* as well as some tissues *in vivo*.[25] In order to investigate the potential for possible clinical therapies, we previously generated a MnSOD plasmid and lipofectin complex (MnSOD-PL),[26,27] which was a FDA-approved therapeutic agent being evaluated in a phase I/II trial for radioprotection of patients with non-small cell lung cancer,[28,29] to target specific tissues or cells.

This study aims to investigate the effects of MnSOD and catalase on HSC engraftment following BM transplant. We first evaluated the ability of MnSOD-PL to enhance the efficiency of HSC transplants, and then determined the intrinsic effect of MnSOD and catalase in HSCs by retroviral transduction. Our results demonstrate that HSC function can be enhanced by ectopic expression of these ROS-detoxifying enzymes, especially after radiation damage.

RESULTS

Basal expression of ROS-detoxifying enzymes in mouse hematopoietic cell subsets

To determine the baseline levels of antioxidant enzymes in HSCs, we first measured the mRNA levels of MnSOD and catalase in the BM-derived HSC and hematopoietic progenitor cell compartments of C57BL/6J mice. To evaluate the expression levels of these enzymes following irradiation, 4 or 8 Gy of ionizing radiation was delivered into each cellular compartment. In the long-term repopulating HSCs, the basal mRNA level of MnSOD was 0.4% and the basal mRNA level of catalase was 1.7%, relative to the β-actin control level. The basal mRNA levels of MnSOD and catalase were two to fourfold higher in the short-term repopulating HSCs than in the long-term repopulating HSCs (**Figure 1a,b**). Irradiation of common myeloid progenitors, common lymphoid progenitors, granulocyte/macrophage progenitors or megakaryocyte/erythrocyte progenitors did not cause an increase in the mRNA expression of MnSOD (**Figure 1a**), but megakaryocyte/erythrocyte progenitor exposure to 8 Gy radiation did cause a substantial increase in the mRNA expression of catalase ($P < 0.05$, **Figure 1b**).

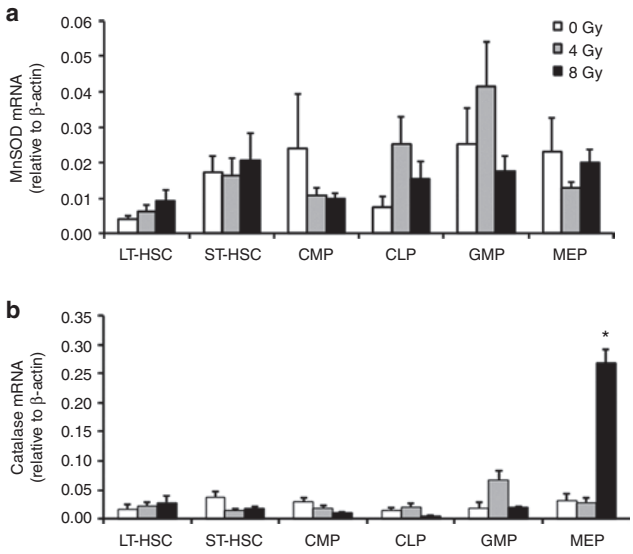

Figure 1 Expression of MnSOD or catalase mRNA in different hematopoietic cell subsets after ionizing radiation. A quantitative analysis of (**a**) MnSOD and (**b**) catalase mRNA levels in C57BL/6J mice was performed with real-time RT-PCR; 4 or 8 Gy of TBI was used for the radiation exposure. Results are normalized to the levels of β-actin. Data are reported as means ± SEM ($n = 3$, $^*P < 0.05$). CLP, common lymphoid progenitor; CMP, common myeloid progenitor; GMP, granulocyte/macrophage progenitor; LT-HSC, long-term repopulating hematopoietic stem cell; MEP, megakaryocyte/erythrocyte progenitor; MnSOD, manganese superoxide dismutase; RT-PCR, reverse transcription-PCR; ST-HSC, short-term repopulating HSC; TBI, total body irradiation.

Beneficial effects of MnSOD-PL on mice transplanted with a limiting dose of HSCs

We hypothesized that a relatively low basal expression level of MnSOD in HSCs would not be sufficient enough to protect HSCs from oxidative stress caused by irradiation, and explored whether administration of MnSOD-PL would confer a protective effect on a limiting dose of HSCs transplanted into lethally irradiated mice. Hence, either the MnSOD-PL, a vector control plasmid lacking the MnSOD gene (mock vector control), or a phosphate-buffered saline (PBS) control was injected 24 hours before total body irradiation (TBI) and BM transplantation (**Figure 2a**). After TBI, 8×10^4 total BM cells (a limiting dose of hematopoietic cells needed for animal survival) were transplanted into lethally irradiated mice and individual mouse survival was followed for 40 days. The mice in both PBS and mock vector control groups began dying 8 days after TBI, and the 30-day survival fractions dropped to 75% in the mock vector control group and 40% in the PBS control group. In contrast, no animals in the MnSOD-PL preconditioned group died from the lethal dose of radiation within 40 days (**Figure 2b**).

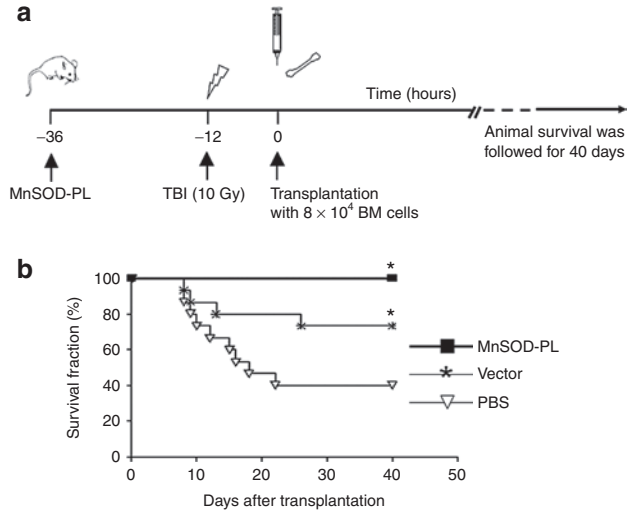

Figure 2 Survival rates of mice transplanted with a limiting dose of BM cells. (**a**) Schematic representation of the experimental design. (**b**) Survival curves of mice following BM transplantation ($n = 15$ per group). There is a significant difference among MnSOD-PL, mock vector control, and PBS control groups ($^*P < 0.05$). BM, bone marrow; MnSOD-PL, manganese superoxide dismutase-plasmid and lipofectin complex; PBS, phosphate-buffered saline; TBI, total body irradiation.

The results demonstrate that MnSOD-PL was able to provide a significant protection for irradiated hosts transplanted with a limiting dose of HSCs. Notably, some protection for irradiated hosts was also observed in the mock vector control group as compared with the PBS control group.

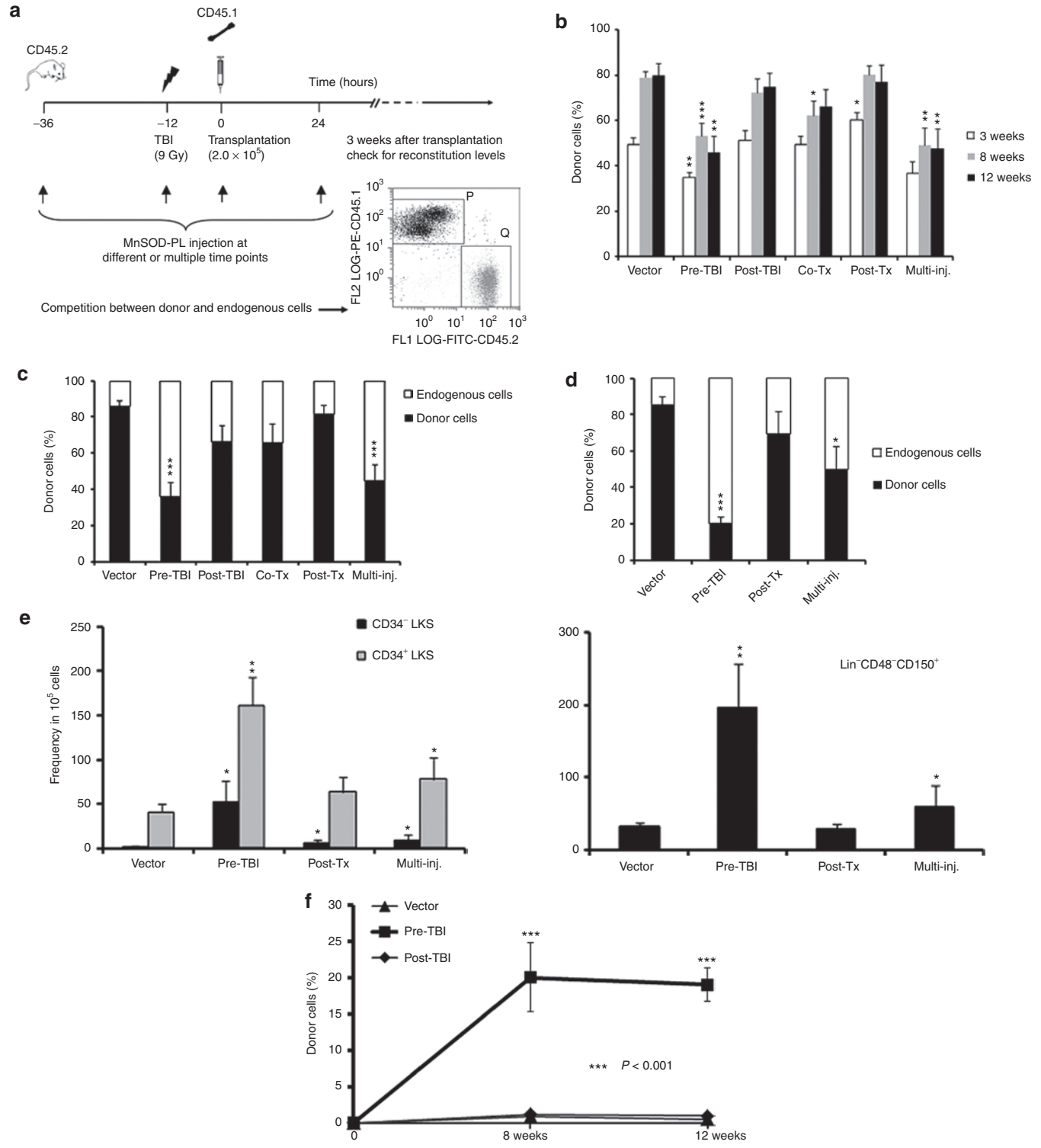

Figure 3 A quantitative analysis of hematopoietic recovery modulated by MnSOD-PL. (**a**) The schematic design of the competitive BM transplant experiment and a representative flow cytometry analysis of competitive engraftment. Peripheral blood engraftment of transplant cells was examined by flow cytometry at (**b**) 3, 8, 12 and (**c**) 24 weeks after transplantation. Vector, mice received empty vector 24 hours before TBI; Pre-TBI, mice received MnSOD-PL intravenously 24 hours before TBI; Post-TBI, mice received MnSOD-PL intravenously immediately after TBI; Co-Tx, mice received MnSOD-PL with the transplanted BM cells; Post-Tx, mice received MnSOD-PL 24 hours after transplantation; Multi-inj., mice received MnSOD-PL at all time points mentioned above ($n = 10$ per group). (**d**) BM engraftment levels of the transplanted cells at 24 weeks after transplantation ($n = 3$–7 per group). (**e**) HSC frequencies in BM ($n = 3$–7 per group). (**f**) Peripheral blood engraftment following secondary transplantation (*$P < 0.05$; **$P < 0.01$; ***$P < 0.001$). BM, bone marrow; HSC, hematopoietic stem cell; MnSOD-PL, manganese superoxide dismutase-plasmid and lipofectin complex; TBI, total body irradiation.

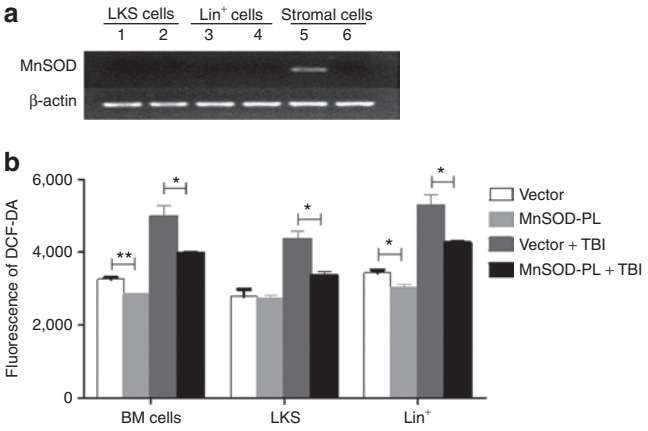

Figure 4 Detection of human MnSOD expression and ROS levels in BM cell compartments of MnSOD-PL–treated mice. (**a**) Expression of human MnSOD mRNAs in different BM cell fractions from the MnSOD-PL– or vector-PL–treated mice measured by RT-PCR. Lanes 1, 3, and 5 represent the samples from the MnSOD-PL–treated mice; lanes 2, 4, and 6 represent the samples from the vector-PL–treated mice. The stromal cells were sorted CD45⁻ adherent cells. (**b**) ROS levels in MnSOD-PL– or vector-PL–treated BM cells detected by flow cytometry. BM cells were harvested 36 hours after MnSOD-PL treatment and 12 hours after TBI. *$P < 0.05$; **$P < 0.01$. BM, bone marrow; DCF-DA, 2′,7′-dichlorofluorescene diacetate; MnSOD-PL, manganese superoxide dismutase-plasmid and lipofectin complex; ROS, reactive oxygen species; RT-PCR, reverse transcription-PCR; TBI, total body irradiation.

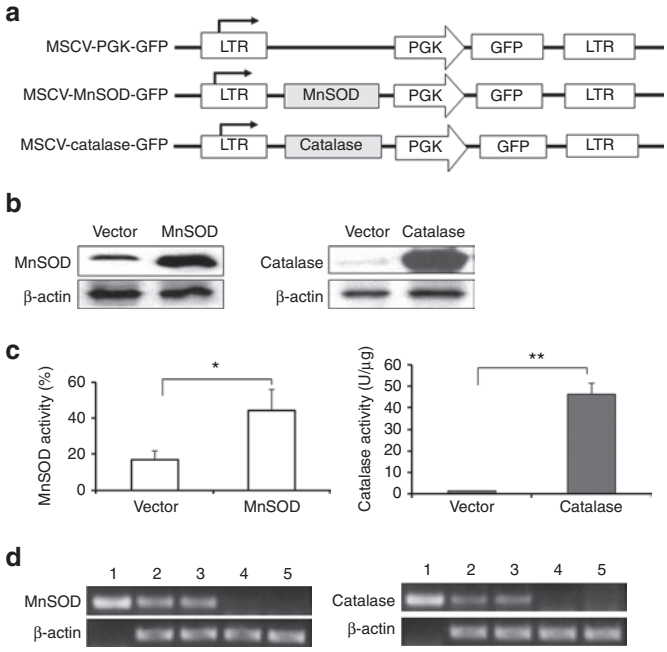

Figure 5 Validations for the functional expression of human MnSOD and catalase retroviral vectors. (**a**) Schematic illustration of retroviral constructs containing MnSOD and catalase genes. (**b**) Representative western blot depicting overexpression of MnSOD (left) and catalase (right) proteins in the transduced AFT024 cells. (**c**) Enzymatic activities of overexpressed MnSOD (left) and catalase (right). Data are presented as means ± SEM (*$P < 0.05$; **$P < 0.01$). (**d**) RT-PCR analysis confirming the expression of human MnSOD or catalase in Lin⁻Sca1⁺ donor cells from the transplanted mice. Lane 1: MnSOD (left) or catalase (right) plasmid sample as the positive control; lanes 2 and 3: two representative samples of MnSOD (left) or catalase (right) transduced Lin⁻Sca1⁺ cells; lanes 4 and 5: two representative samples of vector-transduced Lin⁻Sca1⁺ cells. GFP, green fluorescent protein; LTR, long terminal repeat; MnSOD, manganese superoxide dismutase; MSCV, murine stem cell virus; PGK, phosphoglycerate kinase; RT-PCR, reverse transcription-PCR.

Dissection of hematopoietic regeneration between donor and host cells after MnSOD-PL treatment

To investigate whether the administration of exogenous MnSOD-PL can enhance either donor HSC repopulation (countering the "bystander effect" in the irradiated host) or endogenous hematopoietic recovery in the transplantation recipients after γ-irradiation exposure, we performed a competitive repopulation assay using a suboptimal dose of lethal irradiation (9 Gy). This dose should allow for the survival of some residual HSCs in the host, and in our previous experience, most animals could survive under this condition. The experimental donor cells were transplanted 12 hours after TBI, and the MnSOD-PL was administered at different time points (**Figure 3a**). The level of donor hematopoietic cell engraftment and endogenous hematopoietic recovery within the recipients was monitored for 24 weeks before the transplant animals were killed. The relative contribution of donor versus endogenous hematopoietic cells to the overall hematopoietic recovery in the irradiated recipients was modulated significantly by MnSOD-PL administration, and the modulation patterns were dependent on the specific timing of MnSOD-PL administration. Specifically, when the MnSOD-PL was only administered before TBI (pre-TBI) or at multiple time points (multi-inj., including an injection before TBI), the donor engraftment level was significantly lower than the engraftment level in the mock vector control group, indicating a higher ratio of endogenous hematopoietic cell regeneration (**Figure 3b**). Consistent with this, the engraftment levels of donor cells in the blood (**Figure 3c**) and in the BM (**Figure 3d**) of the pre-TBI or multi-inj. group were much lower than engraftment levels in the mock vector control group at 24 weeks after transplantation (**Figure 3c,d**). However, the donor-derived HSCs, as characterized by the CD34⁻LKS or SLAM phenotype for HSCs, were much more abundant in the pre-TBI or multi-inj. group than in the mock vector control group when quantified by either percentage or absolute yield (**Figure 3e**). This data suggests that although the transplanted HSCs were better preserved, they did not generate proportional progeny in comparison with the endogenous cells.

The repopulation potential of donor HSCs was examined further by a secondary transplant experiment in which donor-derived cells were sorted and re-transplanted with an equal amount of fresh BM competitor cells into lethally irradiated secondary hosts. The peripheral blood engraftment level in the Pre-TBI group was significantly higher than in the mock vector control or post-TBI groups within 12 weeks after transplantation (**Figure 3f**). This data confirms that donor HSCs were better protected from ROS damage and proliferative stress if MnSOD-PL was administered before TBI.

Extrinsic versus intrinsic effects of MnSOD and catalase on hematopoietic cells

To define the "target cells" of the MnSOD-PL treatment, reverse transcription-PCR (RT-PCRs) were performed to detect human MnSOD expression in various BM cell compartments of treated

mice. The results showed that ectopic expression of human MnSOD was only detected in BM CD45$^-$ stromal cells, but not in LKS (Lineage$^-$cKit$^+$Sca1$^+$) cells or Lin$^+$ differentiated cells (**Figure 4a**). To further examine the effect of MnSOD-PL on HSCs, ROS levels were detected by flow cytometry. The results demonstrated that after a challenge of 2 Gy TBI, all BM cell fractions in the MnSOD-PL–treated mice, including LKS cells, Lin$^+$ differentiated cells, and whole BM cells, have significantly reduced ROS levels in comparison with their mock vector control-treated counterparts (**Figure 4b**). These data suggest that a reduction of ROS in HSCs and their progenies by MnSOD-PL was likely through a paracrine action of BM stromal cells or other host cells.

To explore the intrinsic role of elevated ROS-detoxifying enzymes in HSCs, we genetically engineered the HSCs to overexpress human MnSOD and green fluorescent protein (GFP) or human catalase and GFP by retroviral transduction (**Figure 5a**). The efficiency of retroviral transduction was more than 90% in the mouse stromal cell line, AFT024, and 80% in the mouse lineage-depleted BM cells. Western blot results confirmed both enzymes were overexpressed (**Figure 5b**) with correlated enzymatic activities (**Figure 5c**) following transduction. Primary BM Lin$^-$Sca1$^+$ cells were also shown to be successfully transduced with the human MnSOD or catalase (**Figure 5d**). Sorted GFP$^+$ cells were first used for the colony-forming unit (CFU) assay to test the direct effects of these two enzymes on cultured hematopoietic progenitor cells. There was no difference in the number of CFUs identified in each treatment group of the nonirradiated culture plates (**Figure 6a**). However, the CFU-macrophage count in the 2 Gy-irradiated plate was significantly higher in the MnSOD ($P < 0.05$) and catalase ($P < 0.01$) groups than in the mock vector control group (**Figure 6b**). Next, we focused on the long-term repopulating potential of HSCs overexpressing MnSOD or catalase by using a competitive transplant model in which we transplanted various numbers of transduced CD45.1 BM cells into lethally irradiated CD45.2 recipients. We then analyzed peripheral blood for donor cell engraftment and multilineage reconstitution potential by co-staining with antibodies for CD45.1, CD45.2, CD11b, B220, and CD3. At 3 months after transplantation, the relative repopulation activity of donor HSCs in the catalase-transduced group increased by threefold ($P < 0.05$) compared with the vector control, as shown in our previous report,[16] and strikingly, this increased again to 7.5-fold ($P < 0.05$) after 2 Gy re-irradiation (**Figure 6c**). In contrast, a relative increase (1.6-fold) of the repopulation activity of donor HSCs in the MnSOD-transduced group versus the vector control group was not significant ($P > 0.05$) at 3 months after transplantation. However, a significant increase

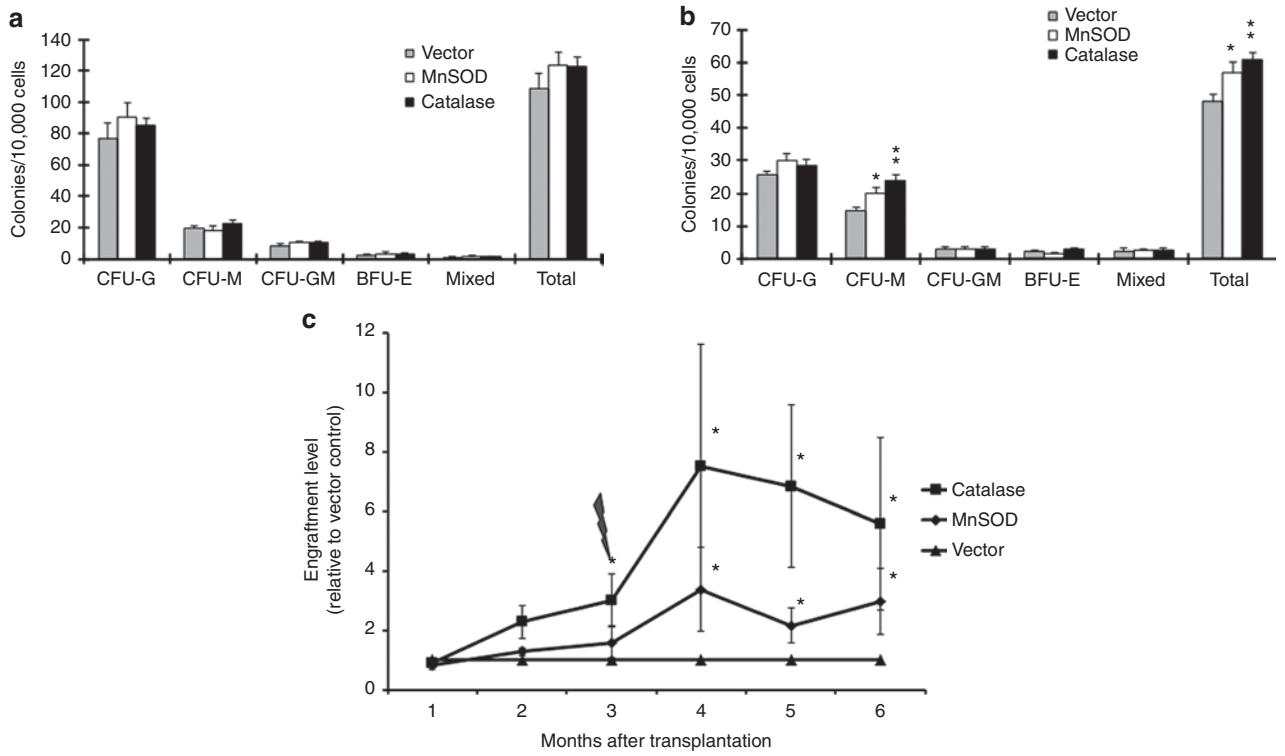

Figure 6 Effects of retrovirus-mediated human MnSOD or catalase on mouse hematopoietic cells *in vitro* and *in vivo*. Sorted GFP$^+$ cells isolated from MSCV-MnSOD-GFP, MSCV-catalase-GFP, or MSCV-GFP–infected BM cells were plated at 4 × 10^4 cells/plate, and CFUs were scored at day 8. (**a**) Colony counts from the nonirradiated cells and (**b**) colony counts from cells that received 2 Gy radiation. Data are presented as means ± SEM of three independent experiments (*$P < 0.05$, **$P < 0.01$). (**c**) Comparison of the donor reconstitution rates in MnSOD, catalase, and mock vector-transduced HSCs following competitive transplantation into 10 Gy-irradiated recipient mice. Three months after transplantation, mice were re-treated with 2 Gy radiation and donor engraftment rates were continually monitored until 6 months after the transplantation. Chart lines represent the ratio of CD45.1$^+$MnSOD$^+$ or CD45.1$^+$catalase$^+$ cells to CD45.1$^+$ mock vector control$^+$ cells in the peripheral blood. Data are presented as means ± SEM of three independent transplantation experiments (n = 13–20 per group, *$P < 0.05$). BFU-E, burst-forming unit-erythroid; BM, bone marrow; CFU-G, colony-forming unit-granulocyte; CFU-GM, colony-forming unit-granulocyte, macrophage; CFU-M, colony-forming unit-macrophage; GFP, green fluorescent protein; MnSOD, manganese superoxide dismutase; MSCV, murine stem cell virus.

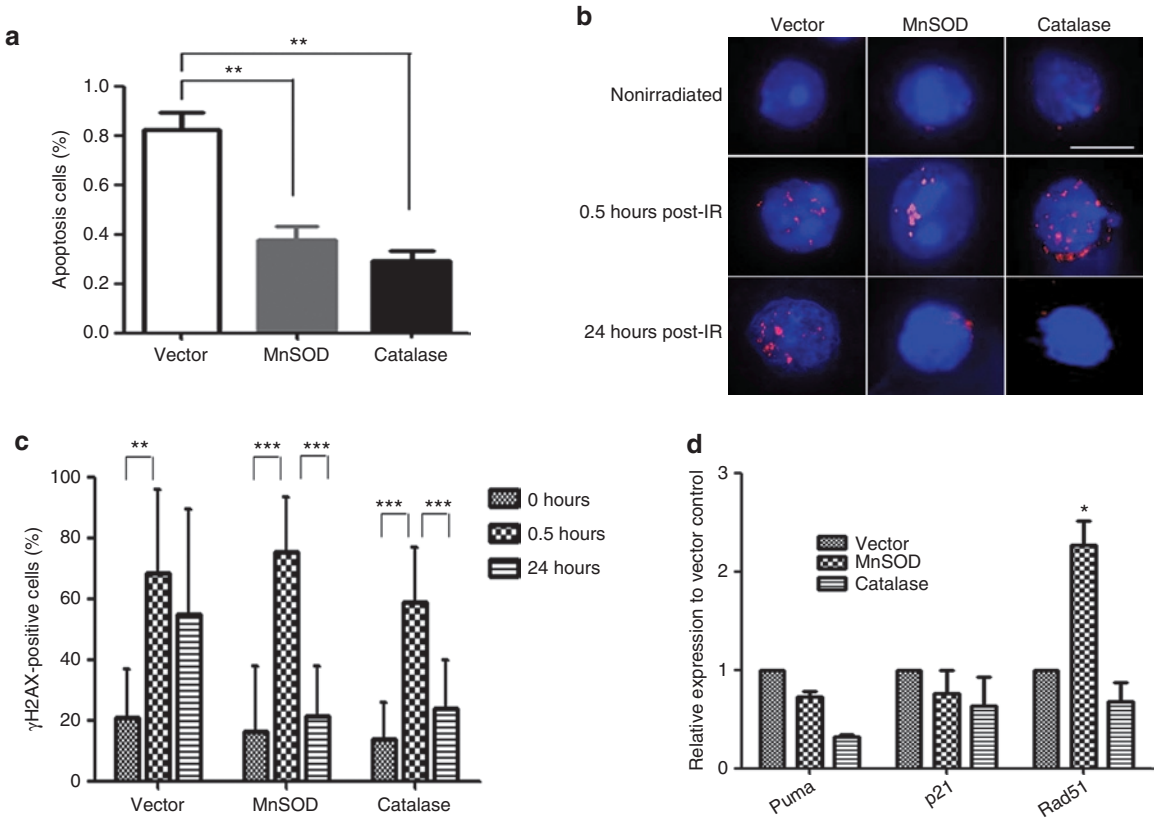

Figure 7 Exploration of the potential cellular and molecular mechanisms. Control vector, MnSOD or catalase retrovirus-transduced LKS cells were repopulated through *in vivo* transplantation and harvested 2 weeks after transplantation for the subsequent analyses below. (**a**) The percentages of apoptotic cells in the MnSOD and catalase groups relative to the vector control group. Data are presented as means ± SEM of three independent transplantation experiments ($n = 15$ per group, $^{**}P < 0.01$). (**b**) Representative images of ionizing radiation-induced foci (IRIF) of γH2AX in nonirradiated or 2 Gy-irradiated vector, MnSOD- and catalase-transduced HSCs after 0.5 and 24 hours (Bar represents 10 μm). (**c**) Quantification of γH2AX-positive cells (≥3 γH2AX foci) in nonirradiated or 2 Gy-irradiated vector, MnSOD- and catalase-transduced HSCs after 0.5 and 24 hours. Unpaired Student's *t*-test was applied to analyze the means ± SD ($^{**}P \leq 0.01$; $^{***}P \leq 0.001$). (**d**) mRNA expression of representative genes related to apoptosis and DNA repair detected by RT-PCR array assays. Data are presented as means ± SEM of three independent experiments ($n = 9$–15 per group; each sample repeated three times; $^{*}P < 0.05$; $^{**}P < 0.01$; $^{***}P < 0.001$). MnSOD, manganese superoxide dismutase; RT-PCR, reverse transcription-PCR.

of 3.4-fold ($P < 0.05$) was observed after a challenge of 2 Gy re-irradiation in the MnSOD group (Figure 6c).

To further explore the underlying cellular and molecular mechanisms, MnSOD- or catalase-transduced LKS cells were examined for cell cycle, apoptosis, and gene expression profiling. While cell cycle analysis did not show significant differences among MnSOD-, catalase-, and vector-transduced LKS cells (data not shown), both MnSOD- and catalase-transduced LKS cells had significantly reduced apoptotic rates compared with the vector control (Figure 7a). γH2AX staining demonstrated that DNA repair was significantly enhanced in the MnSOD- and catalase-transduced LKS cells compared with the vector control (Figure 7b,c). In addition, a quantitative RT-PCR analysis using the "Fluidigm" technology was performed on a limited number of 50 cells. Forty-eight genes related to cell cycle, apoptosis, and redox regulation were selected for the RT-PCR array study. Our results showed that the expression profile of multiple genes was altered significantly in the MnSOD- and catalase-transduced cells compared with the vector control. Especially, Puma, a potent apoptotic gene in the p53 pathway, which was previously shown to mediate the apoptotic effect in HSCs after radiation damage,[30] was significantly downregulated in both MnSOD- and catalase-transduced LKS cells. In contrast, the mRNA expression of p21, a downstream mediator for cell cycle arrest in the p53 pathway, was not altered. In addition, we also observed a significant increase of Rad 51, a DNA repair enzyme, in MnSOD-transduced LKS cells, but interestingly, not in the catalase-transduced cells (Figure 7d). These data will lead our future investigations toward the molecular circuit upon MnSOD or catalase overexpression in HSCs.

DISCUSSION

Our current study provides evidence for radioprotective effects of antioxidant enzymes on HSCs in mice *via* systemic delivery of MnSOD-PL and retroviral transduction of MnSOD or catalase.

Functional studies of MnSOD in HSCs have not been possible due to early lethality of MnSOD knockout mice.[31,32] To circumvent this problem, Friedman and colleagues performed *in vivo* transplantation with fetal liver hematopoietic cells deficient in the MnSOD gene.[33] It was shown that loss of MnSOD resulted in murine hemolytic anemia due to oxidative damage in erythroid progenitor cells, whereas it had no overt effect on lymphoid and myeloid engraftment. Our results indicate that, in mice receiving a

lethal dose of irradiation (10 Gy) followed by BM transplantation using a limiting dose of BM cells, HSC repopulation and animal survival can be dramatically improved by MnSOD-PL administration. While 100% of the mice that received MnSOD-PL survived, a significant nonspecific protective effect was also observed in the mock vector control group when compared with the PBS-treated group. It is possible that lipofectin can induce an immune response when injected into animals, and this immune response may overlap with the function of the delivered genes. According to our data, however, lipofectin by itself did not provide any protection on the irradiated mice when compared with the PBS control (data not shown). Therefore, the nonspecific effect was likely due to the known cofounding effects of the liposome–DNA complex. Noticeably, however, this nonspecific effect did not mask the specific effect of ectopic MnSOD delivered by the injected plasmids when a limiting dose of BM cells was transplanted (**Figure 2b**). A specific effect of human MnSOD was further validated using the competitive repopulation transplant model, in which donor versus host hematopoietic cells were not equally affected and donor HSCs were greatly enriched by MnSOD-PL treatment in comparison with the control plasmid (**Figure 3e**). This potential utility of MnSOD-PL suggests an alternative therapeutic strategy to enhance the HSC engraftment efficiency in BM transplants. Our current study provides a rationale for potential applications of MnSOD-PL in clinical HSC transplantation involving TBI preconditioning regimens, though further studies for optimizing the vector delivery system are still needed.

How MnSOD-PL affects HSCs and their repopulation must be multifactorial. Although our data showed that MnSOD was only detected in BM stromal cells and not in LKS or Lin^+ differentiated cells (**Figure 4a**), ROS levels were significantly reduced in LKS and Lin^+ differentiated cells of MnSOD-PL–treated mice after a low dosage of irradiation (**Figure 4b**). This may indicate a paracrine manner of ROS reduction in HSCs by the MnSOD-PL containing stromal cells. Therefore, MnSOD-PL may affect hematopoietic engraftment largely by influencing the BM niche, rather than by direct effects resulting from its uptake by HSCs. Nevertheless, the subsequent experiments employing retrovirus transductions also support an intrinsic role of ectopic expression of MnSOD or catalase in hematopoietic cells for HSC protection after radiation damage (**Figures 5–7**).

In this study, we demonstrate that retroviral gene transfer of catalase in hematopoietic cells leads to a higher repopulating capacity in competitive BM transplantation when compared to transduction with MnSOD or mock vector control. After an exposure of low-dose irradiation 3 months post-transplantation, the catalase-overexpressing HSCs exhibited an even greater reconstitution capability of up to 7.5-fold in the recipient mice (**Figure 6c**). The catalase enzyme is one of the main regulators of H_2O_2 metabolism, but functional studies of catalase in HSCs have been limited. In one study, Gupta and colleagues demonstrated that in long-term BM cultures with catalase added to the medium, $Lin^-Sca\text{-}1^+$cells accumulated more than 200-fold compared with control cultures.[34] In addition, these cultured cells showed multilineage repopulating activity in lethally irradiated mice, indicating that manipulation of H_2O_2 levels could be used to enhance the growth of HSCs in culture. Proportions of donor-derived $CD45.1^+$ cells at 12 weeks after transplantation were 21.2 ± 11.49–30.5 ± 8.11% in our study. In the study by Gupta *et al.*, proportions were 5.3 ± 0.3–22.6 ± 6.6%. Although cell nature and infused cell dosage were different, our results show that the retroviral catalase gene transfer method is comparable to, but more definitive and significant than, the "expansion" of HSCs in long-term *in vitro* culture.

The differential results obtained following MnSOD or catalase overexpression in hematopoietic cells may be linked to the impact of the enzyme activity level. In our study, the MnSOD protein expression was increased 2.4-fold by retroviral gene transfer, but enzyme activity was increased by only 2.6-fold in the transduced cell line. However, catalase protein expression and activity was increased by 21- and 31-fold, respectively. Oberley and colleagues demonstrated that the tumor-suppressive effect of the MnSOD protein depends largely on its enzyme activity.[35] In addition, MnSOD activity leads to the generation of H_2O_2. H_2O_2 produces a highly toxic hydroxyl radical (·OH) in the presence of reduced metal atoms unless the H_2O_2 is removed by the action of catalase or glutathione peroxidase 1. In this study, the basal mRNA level of catalase was <2–4% relative to β-actin in the long-term and short-term repopulating HSCs. Furthermore, it could not be activated by ionizing radiation. Therefore, overexpression of MnSOD without coactivation of catalase or glutathione peroxidase 1 may be harmful to the cells. Indeed, a number of previous studies have reported that overexpression of MnSOD suppressed cell growth in several types of cancer cells[36–41] and this effect is reversed when the steady state levels of H_2O_2 are decreased by overexpressing catalase.[42]

To explore the underlying mechanisms of enhanced functions of MnSOD- and catalase-transduced LKS cells, additional experiments were performed. Although MnSOD and catalase transductions did not significantly alter the cell cycle parameters, they did reduce the apoptotic rates; γH2AX staining clearly showed that both MnSOD and catalase transductions could potently enhance the DNA repair capability (**Figure 7b,c**). Finally, RT-PCR profiling revealed that MnSOD and catalase transductions could alter the expression of several genes related to apoptosis and DNA repair, namely Puma and Rad51 (**Figure 7d**). Our previous work showed that deletion of Puma in HSCs can confer potent radiation protection,[30] therefore we hypothesize that reduction of Puma in MnSOD- and catalase-transduced LKS cells may be responsible for the enhanced radiation protection (**Figure 7d**). Literature showed that Rad 51 is an important enzyme involved in DNA repair,[43] therefore, a dramatic increase in Rad 51 may be responsible for the enhanced ability of DNA repair in MnSOD-transduced cells (**Figure 7b,c**). While the altered gene expressions may be directly caused by overexpression of MnSOD or catalase in LKS cells, it may also result from feed-back effects of a reduced ROS level, considering ROS itself a signaling molecule. Apparently, more experiments are needed to dissect the precise molecular circuit.

Although our study showed that catalase overexpression alone is sufficient to preserve or augment HSC function even in stressful conditions, greater benefits may be obtained by combining MnSOD and catalase gene transfers in order to maintain low ROS status in the HSCs. Given the fact that multiple antioxidant enzymes are involved in the ROS detoxification,[3] and the function of each enzyme is often cell type-specific, it is necessary to

test other more potent antioxidant enzymes or the combination of these enzymes for their potential application in hematopoietic transplantation as well.

MATERIALS AND METHODS

Mice and cell preparation. C57BL/6J (CD45.2) mice were used for *in vitro* experiments and were used as transplantation recipients, and B6.SJL (CD45.1) mice were used as transplantation donors. For retrovirus transduction, flushed BM cells were depleted of lineage-positive cells at 4 °C with biotin conjugated anti-mouse CD3, CD4, CD8a (T lymphocyte), CD45R (B lymphocyte), Ly-6G (granulocyte), CD11b (macrophage/monocyte), TER-119 (erythroid cell), and streptavidin microbeads (Miltenyi Biotec, Auburn, CA) using a MACS LS column and magnetic cell separator (Miltenyi Biotec). Animal experiments were approved by the Institutional Animal Care and Use Committee of the University of Pittsburgh and the Institute of Hematology, Chinese Academy of Medical Sciences.

Flow cytometry analysis. The following antibodies were used for flow cyotmetry analysis: FITC-CD34, PE-CD45.2, PE-CD127 (IL-7Rα), PEcy5.5-CD45.1 (SJL), a PEcy7-labeled cocktail of antibodies against lineage marker (CD3e, CD4, CD8, B220, CD11b, Gr-1, and TER-119), and biotinylated CD45.2 (eBioscience, San Diego, CA). Purified rat anti-mouse CD16/CD32, PE-Sca1 (Ly-6A/E), PE-TexasRed-CD45R (B220), APC-c-kit (CD117), APC-CD11b, streptavidin-PE, streptavidin-TexasRed, and streptavidin-PEcy7 (BD Pharmingen, San Diego, CA) were also used. The cells were incubated with purified rat anti-mouse CD16/32 to block FcγRII/III before primary antibody incubation. Cells stained with biotinylated antibodies were washed twice with PBS and labeled with streptavidin-PE, streptavidin-TexasRed, or PEcy7. Before analysis, the cells were stained with 4′,6-diamidino-2-phenylindole (DAPI) to select for viable cells. Experiments were performed using a $CyAN_{ADP}$ flow cytometer (DakoCytomation, Carpinteria, CA) and analyzed with Summit v4.3 software (Summit Software, Fort Wayne, IN). ROS levels in MnSOD-PL– or vector-PL–treated BM cells were detected by flow cytometry. Briefly, 100 μg MnSOD-PL or vector-PL was administered into C57BL/BJ (CD45.2) mice *via* tail vein injection. After 24 hours, each mouse received a 2 Gy TBI; 12 hours later, mice were killed and BM cells were harvested. Intracellular ROS levels of whole BM cells, Lin^+ cells, and LKS cells were determined by staining with the probe of 2′,7′-dichlorofluorescene diacetate (DCF-DA) (Invitrogen, Carlsbad, CA).

Retroviral vector construction and transduction. The modified pMSCV-PGK-GFP retroviral vector was a gift from Dr Guy Sauvageau of Université de Montréal. The plasmids containing human MnSOD and catalase cDNA (pRevTRE-MnSOD and pSVZeo-CAT) were a gift from Dr Michael W Epperly. Each cDNA was amplified by PCR reactions and flanked with *EcoRI-BglII* and *HpaI-BglII* sites, respectively. The MnSOD PCR product was then cloned into the pMSCV-PGK-GFP precut with *EcoRI* and *BglII*. For catalase cloning, pMSCV was cut with *EcoRI*, treated with Klenow polymerase for *HpaI* end ligation, and then cut with *BglII*. Each DNA insert was sequenced at the Genomic and Proteomics Core Laboratories of the University of Pittsburgh. For viral transduction, retrovirus particles were produced by cotransfection of HEK 293T cells with each retroviral vector (catalase, MnSOD, or mock vector only) with plasmid vesicular stomatitis virus glycoprotein (pVSVG) and pKat. Supernatants were then collected and used to infect lineage-depleted mouse BM cells or AFT024 stromal cells. For primary BM cell transduction, lineage-depleted cells were pre-stimulated with 50 ng/ml of recombinant mouse stem cell factor, 10 ng/ml of thrombopoietin, and 10 ng/ml of Flt3-ligand (Flt3L) in RetroNectin (Takara Bio, Otsu, Japan) coated 24-well plates. GFP^+ transduced cells were sorted in a MoFlo Sorter (DakoCytomation).

Quantitative RT-PCR. For the quantification of endogenous mouse mRNA of MnSOD and catalase, pooled BM cells from 20 female C57BL/6J (CD45.2) mice (age 6–12 weeks) were stained with a mixture of antibodies against CD34 and a cocktail of lineage markers, Sca1, c-Kit, IL-7Rα, and CD16/CD32 (FcγRII/III), and then sorted into LKS (long-term and short-term), common myeloid progenitors, granulocyte/macrophage progenitors, megakaryocyte/erythrocyte progenitors, and common lymphoid progenitors populations using a FACSAria (Becton Dickinson, Franklin Lakes, NJ) as previously described.[12] After 0, 4 or 8 Gy irradiation, the cells were cultured at 37 °C for 2 hours. Total RNAs were isolated from each cell population using an Absolute RNA Nanoprep kit (Stratagene, Santa Clara, CA). First strand cDNA was synthesized from total RNA using the Superscript First Strand Synthesis system (Invitrogen). Quantitative RT-PCR reactions were performed in a PTC-200 Peltier Thermal Cycler (MJ Research, Waltham, MA) using the DyNAmo HS SYBR Green qPCR Kit according to the manufacturer's instructions (Finnzyme, Espoo, Finland). Three independent reactions were performed using the following program: 1 cycle at 95 °C for 15 minutes and 44 cycles at 94 °C for 15 seconds, 61 °C for 20 seconds, and 72 °C for 20 seconds. For the verification of transduced human MnSOD and catalase gene expression, we sorted Lin^-Sca1^+ BM cells from the transplanted mice. RT-PCR primers used were (5′-3′): GCGGTCGTGTAAACCTCAATAATG and CCAGAGCCTCGTGGTACTTCTC for mouse MnSOD; ACATGGTCT GGGACTTCTGG and CAAGTTTTTGATGCCCTGGTC for mouse catalase; CTGGACAAACCTCAGCCCTA and CTGATTTGGACAAGCA GCAA for human MnSOD; and GCCTGGGACCCAATTATCTT and GAATCT CCGCACTTCTCCAG for human catalase. For the detection of human MnSOD mRNAs in various BM cell fractions of MnSOD-PL– or vector-PL–treated mice, mice were injected with 100 μg MnSOD-PL or vector-PL *via* tail vein injection; 24 hours later, mice were killed and BM cells were isolated. The BM cells were further fractionated into LKS cells, Lin^+ cells and $CD45^-$ stromal cells with magnetic bead separation and FACS, followed by the RT-PCR protocol as described above. For the detection of gene expression profile in the MnSOD- or catalase-transduced LKS cells, the RT-PCR analysis was performed with the BioMark system (Fluidigm, South San Francisco, CA) following the manufacturer's recommended protocol. Data were analyzed using BioMark Real-Time PCR Analysis Software (Fluidigm).

Western blot analysis. To assay for total cellular SOD or catalase protein expression, MnSOD- or catalase-transduced AFT024 cells were sonicated at amplitude 10 for 24 seconds. The sonicated suspensions were centrifuged at 13,000 rpm for 10 minutes at 4 °C. The supernatant was transferred to a new tube, and the protein concentration was measured using the Bio-Rad Protein Assay Reagent (Bio-Rad, Hercules, CA). Denatured protein was resolved by 12% SDS-PAGE and electroblotted onto PVDF transfer membrane (PerkinElmer, Waltham MA). The membrane was incubated with rabbit anti-SOD (1:2,000; Upstate, Billerica, MA), rabbit anti-catalase (1:8,000; Calbiochem, Billerica, MA), or mouse anti-actin polyclonal antibody (1:200; Santa Cruz Biotechnology, Santa Cruz, CA), followed by incubation with horseradish peroxidase conjugated to anti-rabbit or anti-mouse IgG (1:2,500; Santa Cruz Biotechnology). The blots were visualized using Western Lightning Chemiluminescence Reagent Plus (PerkinElmer LAS, Norton, OH).

Enzymatic activity assays. The MnSOD virus-transduced AFT024 cells were sonicated as described above and the supernatant was used to measure MnSOD activity using the MnSOD Assay Kit-WST (Dojindo Molecular Technologies, Rockville, MD) as previously described.[44] Briefly, after adding WST-1 (2-(4-iodophenyl)-3-(4-nitrophenyl)-5-(2,4-disulfophenyl)-2-H-tetrazolium, monosodium salt) and xanthine oxidase working solution to the samples, the microplate was stirred thoroughly and then incubated at 37 °C for 20 minutes. The absorbance at 450 nm was measured using a microplate reader. MnSOD activity was calculated as the percentage of WST-1 formazan inhibition rate by using the following equation: $[[(A_1 - A_3) - (A_S - A_2)]/(A_1 - A_3)] \times 100$, where A_1, A_2, A_3, and A_S were the absorbance at 450 nm for the uninhibited test, blank sample, blank reagent, and

sample, respectively. For catalase activity assay, fresh, sonicated extracts from the catalase-transduced AFT024 cells were used, and catalase activity was measured using the Amplex Red Catalase Assay Kit (Molecular Probes, Carlsbad, CA) according to the manufacturer's protocol. Briefly, the sample was mixed with H_2O_2 solution and incubated for 30 minutes at room temperature. Then, Amplex Red and horseradish peroxidase were added and incubated at 37 °C. After 30 minutes, fluorescence was measured in a fluorescence microplate reader using excitation at 530 nm and emission 590 nm. Catalase concentration was determined by plotting to the catalase standard curve.

CFU assay. For CFU assays, 4×10^3 transduced BM cells were plated in methylcellulose medium (MethoCult M3434; StemCell Technologies, Vancouver, British Columbia, Canada) containing 50 ng/ml of recombinant mouse stem cell factor, 10 ng/ml of recombinant mouse IL-3, 10 ng/ml of recombinant human IL-6 (Peprotech, Rocky Hill, NJ), and 3 U/ml of human erythropoietin at 37 °C with 5% CO_2 and high humidity, and scored for colony formation at 8 and 14 days. To observe the radioprotective effect, 2 Gy radiation was delivered to one set of plates 2 days after the plates were made.

Competitive reconstitution assay and serial transplantation. Six to eight weeks old C57BL/6J (CD45.2) mice or B6.SJL (CD45.1) mice were used as recipients or donors, respectively. We sorted catalase-, MnSOD-, and vector-transduced GFP^+ cells from lineage-depleted donor BM cells and intravenously injected them into 9.5 Gy-irradiated female CD45.2 mice in competition with CD45.1/45.2 double-positive BM mononuclear cells. Three independent transplantations were performed with designated cell doses, and 13–20 mice were used as recipients in each group. Multilineage repopulation of donor myeloid and lymphoid cells was assessed monthly by staining the peripheral blood with antibodies against CD45.1, CD45.2, CD3e, B220, and CD11b. For serial transplantation analysis, we collected $CD45.1^+GFP^+$ donor-derived cells from two $CD45.2^+$ recipient mice 14 weeks after the first BM transplantation and pooled them. A total of 4×10^5 CD45.1 cells from primary recipient marrow, and 1×10^5 $CD45.2^+$ BM cells, were cotransplanted into lethally irradiated (10 Gy) secondary recipient $CD45.2^+$ female mice. Six to eight mice were used as recipients in each group.

Cell cycle and apoptosis analyses. MnSOD, catalase, and vector control retrovirus-transduced Lin^-GFP^+ (CD45.1) mouse BM cells were transplanted into 9.5 Gy lethally irradiated 8-week-old female recipient mice (CD45.2). Each mouse received 2×10^5 cells and five mice were used per group. At 2 weeks after transplantations, recipient mice were killed and BM cells were sorted by flow cytometry for CD45.1 LKS cells; 1×10^4 functional MnSOD, catalase, and vector control-transduced LKS cells, prepared as above, were used for cell cycle and apoptosis analyses by flow cytometry. Briefly, to analyze cell cycle status, the cells were first stained using antibodies against cell surface markers (Lin-APC-CY7, c-kit-APC, and Scal-1-PE-CY7), and then fixed and stained using anti-Ki67 antibody (Pharmingen, San Diego, CA) and Hoechst 33342. To assay apoptosis, cells stained for cell surface markers (Lin-APC-CY7, c-kit-APC, and Scal-1-PE-CY7) were further incubated for 15 minutes with Annexin V and 7-ADD per the manufacturer's protocol using the Annexin V-PE Apoptosis Detection Kit (Pharmingen).

γH2AX staining. 3×10^4 functional MnSOD, catalase, and vector control-transduced LKS cells, prepared as above, were sorted respectively and spun onto slides. The slides were then fixed in 2% paraformaldehyde for 15 minutes, permeabilized by 0.1% Triton X-100 in PBS, and blocked by 1% BSA in PBS for 1 hour at room temperature. The slides were incubated with 1:500 diluted mouse monoclonal antibodies against γH2AX (Abcam, Cambrige, MA) overnight at 4 °C and 1:500 diluted secondary antibodies goat anti-mouse IgG conjugated with Dylight 549 (Multisciences, Lachine, Quebec, Canada) for 1 hour at room temperature the next day. DAPI was used for nuclear staining. Images were produced from an immunofluorescence microscope at ×63 magnification and analyzed for percentage of positive cells containing more than three γH2AX foci. Statistical analyses were performed using GraphPad Prism software (GraphPad Software, La Jolla, CA) and Microsoft Excel. *P* values were calculated using an unpaired two-tailed Student's *t*-test.

ACKNOWLEDGMENTS

This work was supported by grants from the Ministry of Science and Technology of China (2011CB964801, 2010DFB30270, and 2011ZX09102-010), the Natural Science Foundation of China (81090410 and 90913018), and the National Institutes of Health (R01-AI080424) to T.C. T.C. was a recipient of the Scholar Award from the Leukemia & Lymphoma Society (1027-08) and the Outstanding Young Scholar Award from the Natural Science Foundation of China (30825017). This work was also supported by a grant from National Institutes of Health (U19AI68021) to J.G. and the Open Project of the State Key Laboratory of Experimental Hematology of China ZK11-05 to W.M. The authors declared no conflict of interest.

REFERENCES

1. Giles, GI (2006). The redox regulation of thiol dependent signaling pathways in cancer. *Curr Pharm Des* **12**: 4427–4443.
2. Powers, SK, Talbert, EE and Adhihetty, PJ (2011). Reactive oxygen and nitrogen species as intracellular signals in skeletal muscle. *J Physiol (Lond)* **589**(Pt 9): 2129–2138.
3. Kobayashi, CI and Suda, T (2012). Regulation of reactive oxygen species in stem cells and cancer stem cells. *J Cell Physiol* **227**: 421–430.
4. Shao, L, Li, H, Pazhanisamy, SK, Meng, A, Wang, Y and Zhou, D (2011). Reactive oxygen species and hematopoietic stem cell senescence. *Int J Hematol* **94**: 24–32.
5. Boonstra, J and Post, JA (2004). Molecular events associated with reactive oxygen species and cell cycle progression in mammalian cells. *Gene* **337**: 1–13.
6. Li, N and Oberley, TD (1998). Modulation of antioxidant enzymes, reactive oxygen species, and glutathione levels in manganese superoxide dismutase-overexpressing NIH/3T3 fibroblasts during the cell cycle. *J Cell Physiol* **177**: 148–160.
7. Kim, A, Zhong, W and Oberley, TD (2004). Reversible modulation of cell cycle kinetics in NIH/3T3 mouse fibroblasts by inducible overexpression of mitochondrial manganese superoxide dismutase. *Antioxid Redox Signal* **6**: 489–500.
8. Parmar, K, Mauch, P, Vergilio, JA, Sackstein, R and Down, JD (2007). Distribution of hematopoietic stem cells in the bone marrow according to regional hypoxia. *Proc Natl Acad Sci USA* **104**: 5431–5436.
9. Jang, YY and Sharkis, SJ (2007). A low level of reactive oxygen species selects for primitive hematopoietic stem cells that may reside in the low-oxygenic niche. *Blood* **110**: 3056–3063.
10. Ito, K, Hirao, A, Arai, F, Matsuoka, S, Takubo, K, Hamaguchi, I *et al.* (2004). Regulation of oxidative stress by ATM is required for self-renewal of haematopoietic stem cells. *Nature* **431**: 997–1002.
11. Ito, K, Hirao, A, Arai, F, Takubo, K, Matsuoka, S, Miyamoto, K *et al.* (2006). Reactive oxygen species act through p38 MAPK to limit the lifespan of hematopoietic stem cells. *Nat Med* **12**: 446–451.
12. Tothova, Z, Kollipara, R, Huntly, BJ, Lee, BH, Castrillon, DH, Cullen, DE *et al.* (2007). FoxOs are critical mediators of hematopoietic stem cell resistance to physiologic oxidative stress. *Cell* **128**: 325–339.
13. Storz, P (2011). Forkhead homeobox type O transcription factors in the responses to oxidative stress. *Antioxid Redox Signal* **14**: 593–605.
14. Wang, Y, Liu, L, Pazhanisamy, SK, Li, H, Meng, A and Zhou, D (2010). Total body irradiation causes residual bone marrow injury by induction of persistent oxidative stress in murine hematopoietic stem cells. *Free Radic Biol Med* **48**: 348–356.
15. Yahata, T, Takanashi, T, Muguruma, Y, Ibrahim, AA, Matsuzawa, H, Uno, T *et al.* (2011). Accumulation of oxidative DNA damage restricts the self-renewal capacity of human hematopoietic stem cells. *Blood* **118**: 2941–2950.
16. Shen, H, Yu, H, Liang, PH, Cheng, H, XuFeng, R, Yuan, Y *et al.* (2012). An acute negative bystander effect of γ-irradiated recipients on transplanted hematopoietic stem cells. *Blood* **119**: 3629–3637.
17. Deisseroth, A and Dounce, AL (1970). Catalase: Physical and chemical properties, mechanism of catalysis, and physiological role. *Physiol Rev* **50**: 319–375.
18. MILLS, GC (1959). The purification and properties of glutathione peroxidase of erythrocytes. *J Biol Chem* **234**: 502–506.
19. McCord, JM and Fridovich, I (1969). Superoxide dismutase. An enzymic function for erythrocuprein (hemocuprein). *J Biol Chem* **244**: 6049–6055.
20. Weisiger, RA and Fridovich, I (1973). Mitochondrial superoxide simutase. Site of synthesis and intramitochondrial localization. *J Biol Chem* **248**: 4793–4796.
21. Marklund, SL (1982). Human copper-containing superoxide dismutase of high molecular weight. *Proc Natl Acad Sci USA* **79**: 7634–7638.
22. Epperly, MW, Bernarding, M, Gretton, J, Jefferson, M, Nie, S and Greenberger, JS (2003). Overexpression of the transgene for manganese superoxide dismutase (MnSOD) in 32D cl 3 cells prevents apoptosis induction by TNF-alpha, IL-3 withdrawal, and ionizing radiation. *Exp Hematol* **31**: 465–474.
23. Epperly, MW, Osipov, AN, Martin, I, Kawai, KK, Borisenko, GG, Tyurina, YY *et al.* (2004). Ascorbate as a "redox sensor" and protector against irradiation-induced oxidative stress in 32D CL 3 hematopoietic cells and subclones overexpressing human manganese superoxide dismutase. *Int J Radiat Oncol Biol Phys* **58**: 851–861.

24. Southgate, TD, Sheard, V, Milsom, MD, Ward, TH, Mairs, RJ, Boyd, M *et al.* (2006). Radioprotective gene therapy through retroviral expression of manganese superoxide dismutase. *J Gene Med* **8**: 557–565.
25. Zhang, X, Epperly, MW, Kay, MA, Chen, ZY, Dixon, T, Franicola, D *et al.* (2008). Radioprotection *in vitro* and *in vivo* by minicircle plasmid carrying the human manganese superoxide dismutase transgene. *Hum Gene Ther* **19**: 820–826.
26. Greenberger, JS and Epperly, MW (2007). Review. Antioxidant gene therapeutic approaches to normal tissue radioprotection and tumor radiosensitization. *In Vivo* **21**: 141–146.
27. Niu, Y, Wang, H, Wiktor-Brown, D, Rugo, R, Shen, H, Huq, MS *et al.* (2010). Irradiated esophageal cells are protected from radiation-induced recombination by MnSOD gene therapy. *Radiat Res* **173**: 453–461.
28. Greenberger, JS, Epperly, M, Luketich, J, Gooding, W and Belani, CP (2000). Manganese superoxide dismutase-plasmid/liposome (MnSOD-PL) gene therapy protection of the esophagus from chemoradiotherapy damage during treatment of locally unresectable non-small-cell lung cancer (NSCLC). *Clin Lung Cancer* **1**: 302–304.
29. Tarhini, AA, Belani, CP, Luketich, JD, Argiris, A, Ramalingam, SS, Gooding, W *et al.* (2011). A phase I study of concurrent chemotherapy (paclitaxel and carboplatin) and thoracic radiotherapy with swallowed manganese superoxide dismutase plasmid liposome protection in patients with locally advanced stage III non-small-cell lung cancer. *Hum Gene Ther* **22**: 336–342.
30. Yu, H, Shen, H, Yuan, Y, XuFeng, R, Hu, X, Garrison, SP *et al.* (2010). Deletion of Puma protects hematopoietic stem cells and confers long-term survival in response to high-dose gamma-irradiation. *Blood* **115**: 3472–3480.
31. Lebovitz, RM, Zhang, H, Vogel, H, Cartwright, J Jr, Dionne, L, Lu, N *et al.* (1996). Neurodegeneration, myocardial injury, and perinatal death in mitochondrial superoxide dismutase-deficient mice. *Proc Natl Acad Sci USA* **93**: 9782–9787.
32. Li, Y, Huang, TT, Carlson, EJ, Melov, S, Ursell, PC, Olson, JL *et al.* (1995). Dilated cardiomyopathy and neonatal lethality in mutant mice lacking manganese superoxide dismutase. *Nat Genet* **11**: 376–381.
33. Friedman, JS, Rebel, VI, Derby, R, Bell, K, Huang, TT, Kuypers, FA *et al.* (2001). Absence of mitochondrial superoxide dismutase results in a murine hemolytic anemia responsive to therapy with a catalytic antioxidant. *J Exp Med* **193**: 925–934.
34. Gupta, R, Karpatkin, S and Basch, RS (2006). Hematopoiesis and stem cell renewal in long-term bone marrow cultures containing catalase. *Blood* **107**: 1837–1846.
35. Hansen, JM, Zhang, H and Jones, DP (2006). Mitochondrial thioredoxin-2 has a key role in determining tumor necrosis factor-alpha-induced reactive oxygen species generation, NF-kappaB activation, and apoptosis. *Toxicol Sci* **91**: 643–650.
36. Church, SL, Grant, JW, Ridnour, LA, Oberley, LW, Swanson, PE, Meltzer, PS *et al.* (1993). Increased manganese superoxide dismutase expression suppresses the malignant phenotype of human melanoma cells. *Proc Natl Acad Sci USA* **90**: 3113–3117.
37. Li, JJ, Oberley, LW, St Clair, DK, Ridnour, LA and Oberley, TD (1995). Phenotypic changes induced in human breast cancer cells by overexpression of manganese-containing superoxide dismutase. *Oncogene* **10**: 1989–2000.
38. Zhong, W, Oberley, LW, Oberley, TD and St Clair, DK (1997). Suppression of the malignant phenotype of human glioma cells by overexpression of manganese superoxide dismutase. *Oncogene* **14**: 481–490.
39. Liu, R, Oberley, TD and Oberley, LW (1997). Transfection and expression of MnSOD cDNA decreases tumor malignancy of human oral squamous carcinoma SCC-25 cells. *Hum Gene Ther* **8**: 585–595.
40. Li, N, Oberley, TD, Oberley, LW and Zhong, W (1998). Overexpression of manganese superoxide dismutase in DU145 human prostate carcinoma cells has multiple effects on cell phenotype. *Prostate* **35**: 221–233.
41. Weydert, C, Roling, B, Liu, J, Hinkhouse, MM, Ritchie, JM, Oberley, LW *et al.* (2003). Suppression of the malignant phenotype in human pancreatic cancer cells by the overexpression of manganese superoxide dismutase. *Mol Cancer Ther* **2**: 361–369.
42. Rodríguez, AM, Carrico, PM, Mazurkiewicz, JE and Meléndez, JA (2000). Mitochondrial or cytosolic catalase reverses the MnSOD-dependent inhibition of proliferation by enhancing respiratory chain activity, net ATP production, and decreasing the steady state levels of H(2)O(2). *Free Radic Biol Med* **29**: 801–813.
43. Krejci, L, Altmannova, V, Spirek, M and Zhao, X (2012). Homologous recombination and its regulation. *Nucleic Acids Res* **40**: 5795–5818.
44. Zhou, JY and Prognon, P (2006). Raw material enzymatic activity determination: a specific case for validation and comparison of analytical methods–the example of superoxide dismutase (SOD). *J Pharm Biomed Anal* **40**: 1143–1148.